Regulation of postsynaptic AMPA responses by synaptojanin 1

Liang-Wei Gong and Pietro De Camilli[1]

Departments of Cell Biology and Neurobiology, Howard Hughes Medical Institute, and Program in Cellular Neuroscience, Neurodegeneration, and Repair, Kavli Institute of Neuroscience, Yale University School of Medicine, 295 Congress Avenue, New Haven, CT 06510

Contributed by Pietro De Camilli, September 16, 2008 (sent for review July 25, 2008)

Endocytosis of postsynaptic AMPA receptors is a mechanism through which efficiency of neurotransmission is regulated. We have genetically tested the hypothesis that synaptojanin 1, a phosphoinositide phosphatase implicated in the endocytosis of synaptic vesicles presynaptically, may also function in the endocytosis of AMPA receptors postsynaptically. Electrophysiological recordings of cultured hippocampal neurons showed that miniature excitatory postsynaptic current amplitudes were larger in synaptojanin 1 knockout (KO) neurons because of an increase of surface-exposed AMPA receptors. This change did not represent an adaptive response to decreased presynaptic release in KO cultures and was rescued by the expression of wild type, but not catalytically inactive synaptojanin 1, in the postsynaptic neuron. NMDA-induced internalization of pHluorin-tagged AMPA receptors (GluR2) was impaired in KO neurons. These results reveal a function of synaptojanin 1 in constitutive and triggered internalization of AMPA receptors and thus indicate a role for phosphatidylinositol(4,5)-bisphosphate metabolism in the regulation of postsynaptic AMPA responses.

Alzheimer | clathrin | dynamin | endocytosis | long-term depression

Three classes of ionotropic receptors—α-amino-3-hydroxy-5-methylisoxazole-4-propionic acid (AMPA), kainate, and *N*-methyl-D-aspartate (NMDA) receptors—mediate responses to glutamate, the major excitatory neurotransmitter, in the nervous system. AMPA receptors are responsible for most of the fast excitatory synaptic transmission (1). Therefore, alterations in AMPA receptor number and/or function at the synapse are likely to play an important role in synaptic plasticity and in learning and memory. AMPA receptors cycle constitutively by exo-endocytosis between intracellular and surface-exposed pools, and the regulation of this cycle by signal molecules or synaptic activity allows for fast and effective control of receptor number on the postsynaptic membrane (2–5). For example, an increased number of surface-exposed AMPA receptors is a mechanism underlying long-term potentiation. Conversely, long-term depression may involve endocytosis of these receptors to reduce synaptic strength (2–4).

Both constitutive and regulated AMPA receptor endocytosis were shown to be dependent on clathrin, the clathrin adaptors, and dynamin (3, 5–9). Thus, clathrin-mediated endocytosis, a process known to play a fundamental role in the recycling of synaptic vesicles (10, 11), also has a critical role postsynaptically, although the flux of endocytic traffic is much more intense presynaptically. Accordingly, a growing number of components of the clathrin-dependent endocytic machinery of the presynapse were reported, by either morphological or functional studies, to be present also at the postsynapse (8, 9, 12, 13). One protein that is expressed at high levels in the nervous system and is concentrated in nerve terminals, where it has an important role in the clathrin-dependent recycling of synaptic vesicles, is synaptojanin 1 (SJ1) (14–17).

SJ1 is a polyphosphoinositide phosphatase that mediates phosphatidylinositol(4,5)-bisphosphate [$PI(4,5)P_2$] dephosphorylation (14, 15). $PI(4,5)P_2$ is selectively concentrated in the plasma membrane and is a critical coreceptor for the clathrin adaptors and for a variety of other endocytic factors, including actin regulatory proteins (18, 19). After endocytosis, $PI(4,5)P_2$ must be degraded to allow the shedding of these factors. SJ1, which functions in close coordination with dynamin (14, 15, 18), is the enzyme that couples endocytosis to $PI(4,5)P_2$ dephosphorylation (14, 20, 21), thus facilitating clathrin uncoating. In addition, recent studies of SJ1 knockout (KO) neurons have demonstrated that a defect in SJ1 function also results in a partial impairment of synaptic vesicle endocytosis (22), possibly reflecting a role for $PI(4,5)P_2$ turnover during growth and maturation of clathrin-coated pits.

SJ1 comprises 2 distinct inositol phosphatase domains. The central 5-phosphatase domain dephosphorylates $PI(4,5)P_2$ [and also $PI(3,4,5)P_3$] selectively at the 5 position, whereas the N-terminal SacI domain dephosphorylates PI(4)P and also can act on other phosphoinositides (15, 23, 24). Thus, SJ1 can dephosphorylate $PI(4,5)P_2$ to PI. Its C-terminal region interacts with the SH3 domains of a variety of proteins implicated in endocytosis, actin regulation, and signaling, such as endophilin, amphiphysin, syndapin/pacsin, intersectin, nArgBP2, and many others (25–29).

The presence of SJ1 throughout the cell body and dendrites of neurons, albeit at a concentration lower than those in nerve terminals (15, 30), together with the documented importance of clathrin-mediated endocytosis in AMPA receptor trafficking, raise the possibility that SJ1 may also have a function in postsynaptic endocytosis. This hypothesis is supported by the interaction of SJ1 with the postsynaptically enriched protein nArgBP2 (28). Additionally, morphological and biochemical studies of EphrinB–EphB signaling have raised the possibility that the tyrosine phosphorylation of SJ1 by EphB may control postsynaptic endocytosis (31). Finally, it was reported recently that reduced levels of SJ1 suppress the inhibitory effect of the Aβ peptide of the amyloid precursor protein on long-term potentiation induction (32), a phenomenon thought to reflect, at least in part, an increased number of surface-exposed postsynaptic AMPA receptors (2, 3, 5). We have now explored a postsynaptic function of SJ1 using a genetic model—hippocampal neuronal cultures from SJ1-KO mice.

Results

Increased AMPA Miniature Excitatory Postsynaptic Current (mEPSC) Amplitudes in SJ1-KO Neurons. Electrophysiological recordings of cultured hippocampal neurons from wild-type (WT) and SJ1-KO mice revealed that mEPSC amplitudes, known to be mediated by AMPA receptors, were larger in SJ1-KO (23.5 ± 2.1

Author contributions: L.-W.G. and P.D.C. designed research; L.-W.G. performed research; L.-W.G. and P.D.C. analyzed data; and L.-W.G. and P.D.C. wrote the paper.

The authors declare no conflict of interest.

Freely available online through the PNAS open access option.

See Commentary on page 17215.

[1]To whom correspondence should be addressed. E-mail: pietro.decamilli@yale.edu.

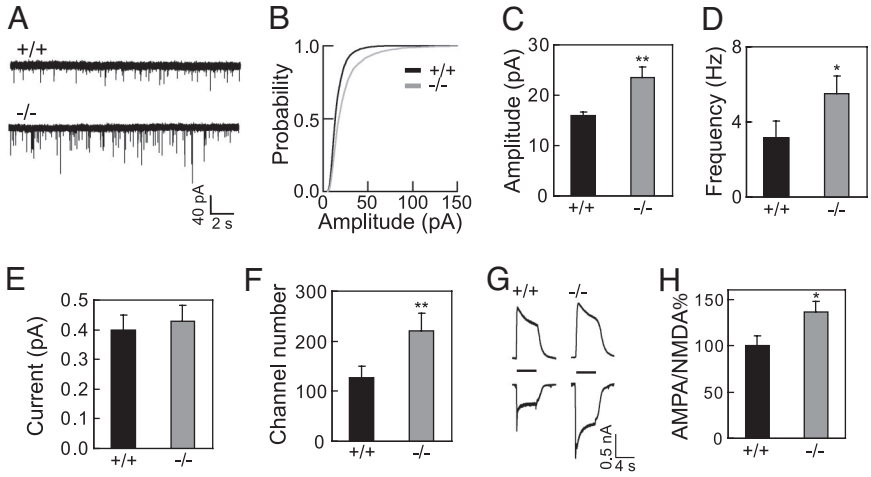

Fig. 1. Increased AMPA mEPSC amplitudes in hippocampal neuron from SJ1-KO mice. (*A*) Typical mEPSC recordings from WT (*Upper*) and SJ1-KO (*Lower*) neurons [14 ays in vitro (DIV)]. (*B*) Cumulative distributions of mEPSC amplitudes for WT and SJ1-KO neurons revealing scaled-up amplitudes in SJ1-KO neurons. (*C*) Average mEPSC amplitudes are increased in SJ1-KO neurons. This increase results in an apparent increase in mEPSC frequency (*D*) due to a higher number of events above threshold. (*E* and *F*) No change in unit channel current of AMPA receptors (*E*), but an increase in the total number of open channels (*F*) in SJ1-KO cells as demonstrated by nonstationary fluctuation analysis. (*G*) Examples of whole-cell AMPA (downward deflections) and NMDA (upward deflections) currents evoked by fast application of 100 μM glutamate to WT and SJ1-KO cells. The currents were recorded in the presence of 500 nM TTX and 50 μM PTX. AMPA currents were recorded by blocking NMDA receptors with 50 μM APV at the holding potential of -60 mV. NMDA currents were recorded in the presence of 10 μM CNQX to block AMPA receptors and 20 μM glycine to activate NMDA receptors at the holding potential of $+60$ mV. (*H*) Statistical analysis showed that the ratio of AMPA/NMDA current is increased in SJ1-KO neurons.

pA, $n = 20$) than in WT (16.0 $\pm$ 0.6 pA, $n = 21$) cells ($P < 0.01$) (Fig. 1 *A–C*). Most likely reflecting this change, the frequency of mEPSCs with amplitudes greater than 5 pA, the threshold used for the analysis, was also increased (SJ1-KO: 5.49 $\pm$ 0.98 Hz, WT: 3.17 $\pm$ 0.85 Hz; $P < 0.05$) (Fig. 1 *A* and *D*). However, both the amplitude (WT: 20.2 $\pm$ 0.9 pA, $n = 15$; SJ1-KO: 20.6 $\pm$ 0.9 pA, $n = 15$; $P > 0.05$) and frequency (WT: 0.80 $\pm$ 0.09 Hz, SJ1-KO: 0.85 $\pm$ 0.14 Hz; $P > 0.05$) of mEPSCs generated by the selective activation of NMDA receptors [as analyzed by the addition of 20 μM glycine, removal of extracellular Mg^{2+}, and blocking of AMPA receptors with 10 μM 6-cyano-7-nitroquinoxaline-2,3-dione (CNQX)] were the same in the 2 genotypes. Therefore, the increase in frequency observed for AMPA mEPSCs is only apparent and reflects the more frequent occurrence of events above the 5-pA threshold. No difference between WT and SJ1-KO neurons was observed in AMPA mEPSC rise time (WT: 1.90 $\pm$ 0.07 ms, SJ1-KO: 1.75 $\pm$ 0.07 ms; $P > 0.05$) or decay time (WT: 2.74 $\pm$ 0.09 ms, SJ1-KO: 2.57 $\pm$ 0.11 ms; $P > 0.05$).

A selective increase of AMPA mEPSC amplitude, but not NMDA mEPSC amplitude, in SJ1-KO neurons suggested a postsynaptic locus of the change. This was further confirmed by the "rescue" of these changes via the selective expression of SJ1 in the postsynaptic neuron (see below). The change in AMPA responsiveness of the postsynapse could be explained by an increase in either the conductance of individual AMPA receptors or their total number. We next used nonstationary fluctuation analysis (33) to distinguish between the 2 possibilities. For a given postsynaptic cell, we obtained the average mEPSC and then scaled individual mEPSCs to the peak of this event. This allowed us to obtain a mean-versus-variance curve of mEPSCs and to estimate the single-channel current and the number of channels involved in each mEPSC. The average single-channel current was not different between WT (0.40 $\pm$ 0.05 pA, $n = 17$) and SJ1-KO (0.43 $\pm$ 0.05 pA, $n = 17$) neurons ($P > 0.05$) (Fig. 1*E*). However, the estimated number of open channels was increased by $\approx$70% in SJ1-KO neurons (WT: 127 $\pm$ 22, SJ1-KO: 221 $\pm$ 35; $P < 0.01$) (Fig. 1*F*), suggesting an increased number of AMPA receptors at the synapse.

Rapid application of 100 μM glutamate was used to determine whether overall AMPA responses (i.e., effects involving both synaptic and nonsynaptic receptors) also were altered in SJ1-KO neurons. AMPA responses were larger in SJ1-KO cells (SJ1-KO: 4.33 $\pm$ 0.44 nA, $n = 21$; $P < 0.01$) than in WT cells (WT: 2.83 $\pm$ 0.27 nA, $n = 21$), whereas NMDA responses were similar in the 2 genotypes (WT: 2.98 $\pm$ 0.25 nA, $n = 21$; SJ1-KO: 3.38 $\pm$ 0.29 nA, $n = 21$; $P > 0.05$) (Fig. 1*G*). As a result, the ratio of AMPA/NMDA current increased by 35% in SJ1-KO neurons (WT: 100 $\pm$ 10.5%, $n = 21$; SJ1-KO: 136 $\pm$ 12%, $n = 21$; $P < 0.05$) (Fig. 1*H*). Collectively, these results are consistent with an impaired endocytosis of AMPA receptors, and thus with an increased number of AMPA receptors in the plasma membrane.

The Increase in mEPSC Amplitude Is Not Due To Altered Presynaptic Activity. Previous studies of cultured hippocampal neurons have shown that the number of AMPA receptors present in the postsynaptic membrane may vary as a function of presynaptic activity and that this plasticity plays an important role in maintaining synaptic homeostasis (34). Since transmission at synapses of SJ1-KO neurons depresses faster and more intensely than in WT during prolonged stimulation (14, 35), the increase in postsynaptic AMPA receptor number at SJ1-KO synapses may represent an adaptive response to a change in presynaptic function, rather than to a primary postsynaptic defect. To test this hypothesis, mEPSCs of WT and SJ1-KO neurons were measured after a prolonged but reversible block of synaptic transmission. Under these conditions, any difference resulting from a change in presynaptic release should be abolished.

Blockage of synaptic transmission via chronic exposure to AMPA receptor inhibitors (for example, CNQX) or to the Na^+ channel blocker tetrodotoxin (TTX) produces an increase in mEPSC frequency and amplitude (36) that correlates with an increase in the size of the synapse and of its docked synaptic vesicle pool (37). In agreement with these previous studies, analysis of AMPA responses following a 40-h treatment with CNQX demonstrated a strong increase in mEPSC frequency in both WT (control: 1.70 $\pm$ 0.40 Hz, $n = 24$; CNQX: 2.97 $\pm$ 0.48 Hz, $n = 23$; $P < 0.05$) and SJ1-KO (control: 3.15 $\pm$ 0.54 Hz, $n =$

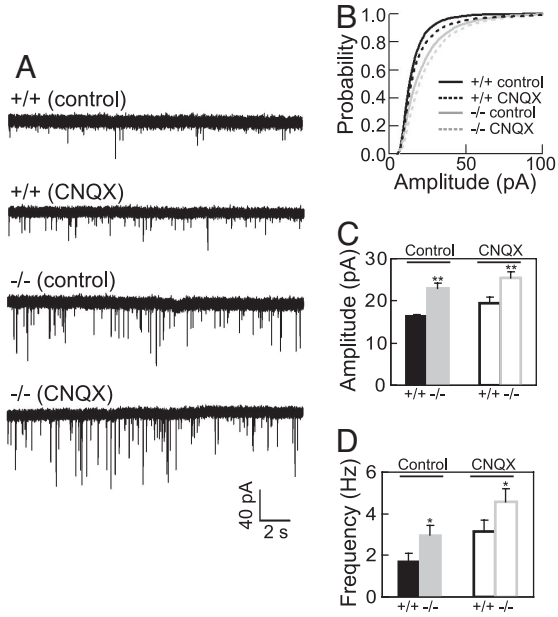

Fig. 2. Increased AMPA receptor responses are not due to altered presynaptic activity in SJ1-KO neurons. (*A*) The mEPSC recording from WT and SJ1-KO neurons (14 DIV) preincubated for 40 h in either control conditions or in the presence of 10 μM CNQX. (*B*) Cumulative distributions of mEPSC amplitudes demonstrating that CNQX pretreatment increases mEPSC amplitude in both WT and SJ1-KO neurons. (*C* and *D*) Barograms showing a statistically significant increase of amplitude (*C*), and therefore also of apparent frequency (*D*), in SJ1-KO neurons relative to WT both in control and CNQX-treated cultures, thus proving that altered presynaptic activity cannot account for the increased mEPSC amplitude in SJ1-KO neurons.

22; CNQX: 4.59 ± 0.62 Hz, $n = 21$; $P < 0.05$) neurons (Fig. 2 *A* and *D*). Prolonged exposure to CNQX also caused a small increase in mEPSC amplitude in both WT (control: 16.3 ± 0.5 pA, CNQX: 19.4 ± 1.5 pA; $P < 0.05$) and SJ1-KO (control: 22.9 ± 1.3 pA, CNQX: 25.5 ± 1.5 pA; $P > 0.05$) neurons, although the increase in SJ1-KO neurons was not statistically significant (Fig. 2 *A–C*).

Importantly, even in cultures chronically blocked with CNQX, significantly larger mEPSC amplitudes were observed in SJ1-KO than in WT neurons (CNQX-treated WT: 19.4 ± 1.5 pA, CNQX-treated SJ1-KO: 25.5 ± 1.5 pA; $P < 0.05$) (Fig. 2 *A–C*). Thus, the increased amplitude of mEPSCs in SJ1-KO neurons does not result from altered presynaptic activity. Most likely, it reflects a role of SJ1 in controlling the pool of AMPA receptors at the surface of the postsynaptic cell.

Transfection of SJ1 in SJ1-KO Neurons Restores Normal mEPSC Amplitudes. To provide a direct demonstration that the changes in mEPSC amplitude were due to the lack of SJ1 in the postsynaptic cell, "rescue" experiments were performed. To this aim, both major splice variants of SJ1—SJ1–145 and SJ1–170 (15)—were transfected into cultured SJ1-KO hippocampal neurons using the pIRES2-GFP vector. This vector induces the independent expression of GFP, thus allowing the identification of transfected neurons. The shorter splice variant, SJ1–145, is the isoform that by far predominates in the adult nervous system, where it is concentrated at synapses (15). The longer splice variant, SJ1–170, which comprises an additional 30-kDa C-terminal extension, predominates early in the developing nervous system and represents a housekeeping isoform present at low levels in most cell types (15, 38). Expression in SJ1-KO neurons of either SJ1–145 or SJ1–170, but not of GFP alone, restored mEPSC amplitude to normal values

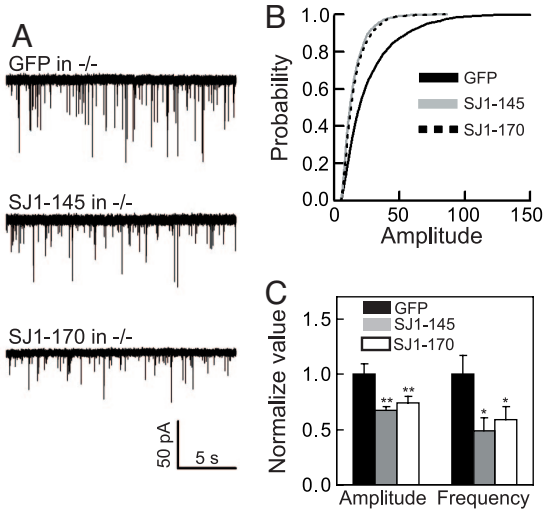

Fig. 3. Both SJ1–145 and SJ1–170 revert the increase in mEPSC amplitude observed in SJ1-KO neurons. (*A*) Representative example of mEPSC traces recorded from SJ1-KO neurons expressing GFP alone or GFP together with either SJ1–145 or SJ1–170. (*B*) Cumulative distributions of mEPSC amplitudes showing that both SJ1–145 and SJ1–170 scale down mEPSC amplitude in SJ1-KO neurons, relative to neurons expressing GFP only. (*C*) Statistical analysis shows that both mEPSC amplitude and frequency were decreased in neurons expressing either SJ1–145 or SJ1–170 relative to neurons expressing GFP only.

(SJ1–145: 15.8 ± 1.0 pA, $n = 17$, $P < 0.01$; SJ1–170: 17.4 ± 1.4 pA, $n = 16$, $P < 0.01$; GFP: 23.5 ± 2.0 pA, $n = 16$) (Fig. 3). Correspondingly, the frequency of mEPSCs greater than 5 pA, the threshold used for the analysis, also was restored to normal levels in cells transfected with either SJ1 isoform (SJ1–145: 1.42 ± 0.34 Hz, $P < 0.05$; SJ1–170: 1.69 ± 0.35 Hz, $P < 0.05$; GFP: 2.87 ± 0.51 Hz) (Fig. 3 *A* and *C*). Because only a few cells in each culture were transfected with the protocol used (typically <1%), most inputs to these cells originate from nontransfected neurons. Thus, these experiments also indicate very strongly that the rescue occurs by the expression of SJ1 in the postsynaptic cell.

The Phosphatase Activity of SJ1 Is Required for Normal mEPSC Amplitude. Next, the importance of the phosphatase activity of SJ1 in regulating AMPA responsiveness of the postsynaptic cell was investigated. A mutant SJ1–145 construct (mtSJ1–145) harboring 2 point mutations that impair the catalytic activity of the Sac1 (C383S) and 5-phosphatase (D730A) (22) modules, respectively, was generated. Control experiments confirmed the complete loss of enzymatic activity of mtSJ1–145 (22). Electrophysiological recordings showed that SJ1-KO neurons expressing WT SJ1–145 had smaller mEPSC amplitudes (19.3 ± 1.8 pA, $n = 16$) than neurons expressing mtSJ1–145 (26.1 ± 1.9 pA, $n = 16$; $P < 0.01$) (Fig. 4 *A* and *B*), thus confirming the critical role of the catalytic activity of SJ1 in controlling postsynaptic AMPA responses. Accordingly, neurons expressing WT SJ1–145 also displayed an apparently lower mEPSC frequency (events with a threshold higher than 5 pA) (SJ1–145: 3.01 ± 0.69 Hz, mtSJ1–145: 6.09 ± 1.34 Hz; $P < 0.05$) (Fig. 4 *A* and *C*).

NMDA-Induced Internalization of AMPA Receptors Is Inhibited in SJ1-KO Neurons. We then used pH-GluR2, a chimeric protein comprising ecliptic pHluorin (39) fused to the N-terminal extracellular domain of the GluR2 (40), to examine the effect of the lack of SJ1 on the endocytosis of AMPA receptors. pHluorin is a pH-sensitive mutant of the green fluorescence protein. When excited with 488 nm light, pH-GluR2 undergoes a major

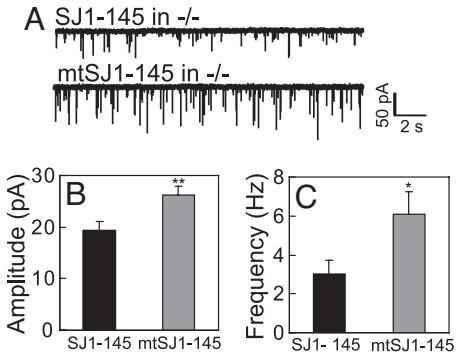

Fig. 4. The phosphatase activity of SJ1 is necessary to restore normal mEPSC amplitude in SJ1-KO mice. (*A*) Traces from SJ1-KO neuron expressing either WT SJ1–145 or a mutant SJ1–145 lacking both the Sac1 and the inositol 5-phosphatase activities (mtSJ1–145) demonstrate smaller mEPSC amplitudes in cells transfected with WT SJ1–145. (*B* and *C*) Statistical analysis of mEPSCs, showing reductions in mEPSC amplitude (*B*) and apparent frequency (*C*) in SJ-KO neurons expressing SJ1–145 relative to SJ1-KO neurons expressing mtSJ1–145.

decrease in fluorescence as it translocates from the neutral pH (≈7.4) of the extracellular medium to the acidic (pH < 6.0) pH of endosomes (39, 40). Thus, changes in the fluorescence intensity of pH-GluR2 report the endocytosis of this chimeric glutamate receptor (39, 40).

In WT neurons, application of NMDA for 5 min produced a strong attenuation of fluorescence intensity in the dendrites (0.45 ± 0.06 reduction, $n = 8$) (Fig. 5), which was more prominent in dendritic shaft, consistent with previous reports (40). In SJ1-KO neurons, the reduction in fluorescence intensity induced by NMDA application was significantly smaller (0.20 ± 0.02 reduction, $n = 8$; $P < 0.05$) (Fig. 5). Thus, AMPA receptor endocytosis induced by NMDA involves SJ1.

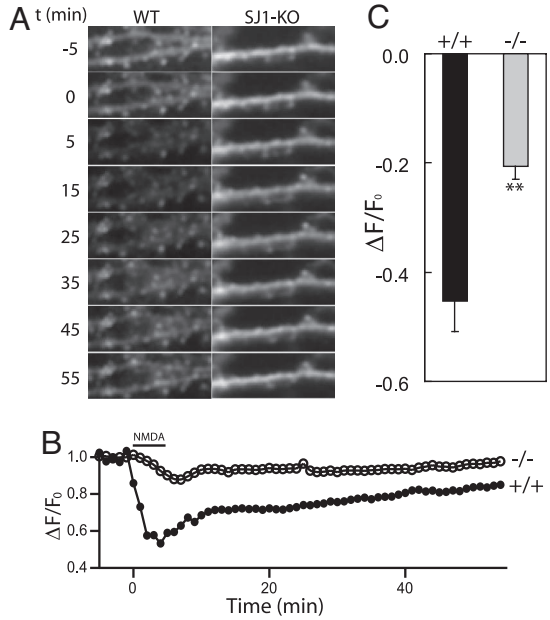

Fig. 5. Internalization of AMPA receptors following the application of NMDA is impaired in SJ1-KO neurons. (*A*) Time traces of pH-GluR2 fluorescence in WT and SJ1-KO neurons in response to a 5-min NMDA application. (*B*) Time course of pH-GluR2 fluorescence in the fields shown in *A*. (*C*) Average reduction of the pH-GluR2 fluorescence signal in dendrites of WT and SJ1-KO neurons at the end of the 5-min NMDA application. The decrease in fluorescence intensity is lower in mutant neurons.

Discussion

Our results demonstrate that lack of SJ1 in hippocampal neurons results in an increase in mEPSC amplitude at excitatory synapses that can be attributed to an increase in the number of surface AMPA receptors by nonstationary fluctuation analysis. This increase is not limited to AMPA receptors localized at the synapse, as shown by AMPA responses induced by puffs of glutamate, thus suggesting that the change is not explained by a modified equilibrium between synaptic and extrasynaptic receptors.

Several considerations indicate that the increase in mEPSC amplitude observed in SJ1-KO neurons is not likely to result from decreased presynaptic efficiency in SJ1-KO cultures. First, the increase persisted in cultures that had been exposed to a prolonged preincubation with the AMPA receptor inhibitor CNQX to induce a chronic block of synaptic activity. Second, no obvious differences in mEPSC dynamics, including rise time and decay time, were observed between WT and SJ1-KO neurons. In contrast, previous studies have demonstrated that following chronic blockage of AMPA receptor responses with NBQX (an analogue of CNQX), mEPSCs have faster dynamics due to a modified contribution of specific AMPA receptor isoforms (greater contribution of GluR1 homomers) to AMPA-mediated currents (36). Third, and most importantly, changes in the amplitude of AMPA mEPSCs observed in SJ1-KO neurons were rescued by the selective expression of SJ1 in postsynaptic cells.

A major mechanism underlying the control of synaptic strength is the net balance between the continuous delivery to (by exocytosis) and removal from (by endocytosis) the postsynaptic membrane of AMPA receptors (2, 4, 5). This exo-endocytic recycling occurs continuously, largely independently of synaptic activity (4, 41). In view of the strong evidence linking SJ1 to the endocytic pathway (14, 16, 17, 22), the increase in mEPSC amplitude observed in SJ1-KO neurons is likely to be explained, at least in part, by a defect in the endocytic limb of this cycle. This possibility is strongly supported by the impaired NMDA-dependent internalization of pH-GluR2 observed in these neurons.

The formation of a clathrin-coated endocytic pit is triggered by the binding of clathrin adaptors to the membrane in a process involving both $PI(4,5)P_2$ and membrane proteins (14, 18, 42). Dephosphorylation of $PI(4,5)P_2$ by SJ1 and other phosphatases is critical to promote shedding of the clathrin coat immediately after fission, and perturbation of SJ1 function produces a delay of recycling membranes at a postendocytic stage (14, 21). In addition, recent studies of exo-endocytosis in the presynaptic compartment suggest that lack of SJ1 also inhibits, at least partially, the internalization reaction of endocytosis (22). A similar role in endocytosis was reported for synaptojanin 2 (43), a homologue of SJ1 that is expressed at much lower levels than SJ1 in the nervous system. This inhibition may reflect sequestration of endocytic factors on postendocytic membranes, with a resulting reduction in their availability to initiate new endocytic events. Alternatively, as some studies suggest, it may be due to a need for a dynamic cycle of $PI(4,5)P_2$ synthesis and dephosphorylation on the plasma membrane during the growth of a clathrin-coated pit (20). Thus, it is plausible that a defect in endocytosis may underlie the enhanced mEPSC amplitude in SJ1-KO neurons.

A role for SJ1 in the postsynaptic endocytic pathway is in good agreement with the large body of evidence indicating major functional similarities between presynaptic and postsynaptic endocytic mechanisms. In this respect, the reported postsynaptic role of dynamin isoforms (12, 44) is of special interest, because SJ1 was identified as a ligand for many of the same proteins that also bind dynamin (15, 26, 27, 29). We also note that a major SJ1-

and dynamin-interacting protein, nArgBP2, is a postsynaptically enriched scaffold protein (28).

Additional mechanisms through which lack of SJ1 may mediate enhanced AMPA responsiveness—i.e., mechanisms independent of changes in endocytosis—may come into play. For example, $PI(4,5)P_2$ is a major regulator of actin nucleation (18), and the increase in neuronal $PI(4,5)P_2$ levels (about 60%) resulting from the absence of this protein (14) may produce changes in actin dynamics within dendritic spines. These changes, in turn, may affect synaptic structure and function with indirect affects on AMPA receptor responses (18).

Two previous observations are particularly noteworthy in the context of our findings. The first is that SJ1 was proposed to be a key component of the signaling pathway that mediates the modulatory effect of the EphrinB–EphB-2 system on the endocytosis of AMPA receptors triggered by both NMDA and AMPA applications. SJ1 is a physiological substrate for the tyrosine kinase activity of the EphB2 receptors, and SJ1 mutants that cannot be phosphorylated by EphB have a dominant negative effect on these endocytic reactions (31). Our results provide genetic evidence supporting this hypothesis. The second is that SJ1 is an important physiological binding partner of endophilin (26, 29) which, in turn, is a major interactor of Arc. Arc, a protein whose induction is strongly stimulated by synaptic activity, down-regulates AMPA responses by promoting AMPA receptor endocytosis (45).

SJ1 is a prominent substrate for calcineurin, a Ca^{2+}-dependent serine–threonine phosphatase. The action of calcineurin reverses an inhibitory constitutive phosphorylation of SJ1 at rest and promotes its endocytic function upon synapse stimulation (30, 46). The observation that NMDA application activates calcineurin and that the stimulatory effect of NMDA application on AMPA receptor endocytosis is blocked by calcineurin antagonists (47) is consistent with a model in which postsynaptic SJ1 is involved in mediating some of the effects of NMDA receptor activation. Interestingly, a recent study showed that decrease of $PI(4,5)P_2$ is required to trigger internalization of AMPA receptors in response to NMDA activation, and that inhibition of PLC, another manipulation that enhances $PI(4,5)P_2$ levels, impairs NMDA-induced AMPA receptor internalization and long-term depression (48).

Finally, our findings may have implication in the field of Alzheimer's disease. It was reported that amyloid-β peptide implicated in Alzheimer's disease induces synaptic dysfunction at least in part by triggering the internalization of AMPA receptors (49). It is, therefore, of interest that decreased expression of SJ1 suppresses the inhibiting effect of this peptide on long-term potentiation (32). Conversely, excess of SJ1, as it occurs in Down's syndrome patients as a consequence of the triplication of the SJ1 gene, correlates with early-onset Alzheimer's diseases in these patients (50). Although increased expression of the amyloid precursor protein, whose gene also is triplicated in Down's syndrome, is likely to play a major role in early-onset Alzheimer's disease, increased SJ1 function may synergize with the actions of amyloid-β peptide on AMPA in inducing AMPA receptor internalization.

Materials and Methods

Neuronal Cultures and Transfection. Primary hippocampal neuronal cultures were prepared as described (51) from newborn littermates derived from the mating of mice heterozygous for the SJ1 null mutation (14). Transfections were carried out at 3–5 DIV in 24-well plates using 1.5 μg DNA per well and Lipofectamine 2000 (Invitrogen). Following 3–5 h of exposure to Lipofectamine, coverslips were washed thoroughly and returned to the original culture medium until used.

Cloning of SJ1 in the pIRES2-GFP Vector. The pIRES2-GFP-SJ1–170 was cloned in 2 steps. First, the N-terminal portion of the SJ1 cDNA was obtained by PCR from our pcDNA-FLAG-SJ1–170 plasmid by using a 5′ primer that added an NheI site to the 5′ end of the gene and a 3′ primer that encoded the EcoRI site at nucleotide 339. This PCR product and the pIRES2-GFP vector (Clontech) were digested with NheI and EcoRI and then ligated to produce a pIRES2-GFP-N-terminal SJ1 construct. Next, pcDNA-FLAG-SJ1–170 (which has both an internal and a C-terminal EcoRI site) and pIRES2-GFP-N-terminal SJ1 were digested with EcoRI alone, and the SJ170 fragment was ligated into the pIRES2-GFP-N-terminal SJ1 vector.

The pIRES2-GFP-SJ145 was obtained by digesting both pIRES2-GFP-SJ170 and pGEX SJ1–145-PRD (encoding a fusion protein of the proline-rich domain of SJ1–145; ref. 15) with SpeI and SalI. The pIRES2-GFP-SJ1–145 was generated by ligation of the resulting fragments.

Electrophysiology. Whole-cell patch clamp recordings of mEPSC were performed on 13–16 DIV primary hippocampal neuronal cultures. During recordings, neurons were continuously perfused with an extracellular solution containing (in mM) 140 NaCl, 3 KCl, 2 $CaCl_2$, 2 $MgCl_2$, 10 Hepes, and 20 glucose, buffered to pH 7.3 with NaOH. The intracellular solution present in the pipette contained (in mM) 115 $CsMeSO_4$, 20 CsCl, 10 Hepes, 0.6 EGTA, 2.5 $MgCl_2$, 0.4 Na_3GTP, 4 Na_2ATP, and 10 sodium phosphocreatine. A concentration of 50 μM picrotoxin (PTX) was used to block inhibitory synaptic transmission, and 500 nM TTX was used to block the generation of action potentials. NMDA mEPSCs were recorded at -60 mV in the extracellular solution described above but lacking $MgCl_2$ and containing 10 μM CNQX to block AMPA receptors and 20 μM glycine to activate NMDA receptors. Whole-cell AMPA and NMDA currents evoked by fast application of 100 μM glutamate for WT and SJ1-KO cells were recorded in the presence of 500 nM TTX and 50 μM PTX. AMPA current was recorded by blocking NMDA receptors with 50 μM APV at the holding of -60 mV, and NMDA current was recorded with 10 μM CNQX to block AMPA receptors and 20 μM glycine to activate NMDA receptor at the holding potential of $+60$ mV.

Recordings were acquired with an EPC-9 amplifier (HEKA). Glass electrodes (Hilgenberg) were pulled with a Sutter P-97 micropipette puller (Sutter Instruments) to a tip resistance of 2–3 MΩ. Data were filtered at 1 kHz, digitized at 2 kHz, and analyzed using the Mini Analysis Program (Synaptosoft). The threshold of mEPSC amplitude was set at 5 pA. The holding potential was -60 mV. Series resistance (R_S) during whole-cell recordings was not compensated, and recordings with R_S greater than 20 MΩ were not included in the analysis. Data were initially pooled into 3 separate genotype groups (WT, HT, and SJ1-KO). Data from WT (15.4 $\pm$ 0.9 pA, $n = 17$) and HT (16.4 $\pm$ 0.7 pA, $n = 16$; $P > 0.05$) were then pooled together because no significant difference was observed between WT and HT recordings.

Nonstationary Noise Analysis. Nonstationary noise analysis was performed as described previously (33). The baseline variance was measured from a postevent current and subtracted from the total variance. The variance was plotted against mean amplitude (i), binned, and the relationship variance = $iI - i^2/N$ was fit (least-squares method) to the data points to obtain I, the single-channel unitary current, and N, the number of channels responsible for generating mEPSCs. All statistical results are given as average $\pm$ SEM, and the significance was evaluated using *t* tests or 1-way ANOVA. * indicates $P < 0.05$, and ** indicates $P < 0.01$.

pH-GluR2 Imaging Experiments. All imaging experiments were performed at room temperature using a Leica DMI 6000B system. pHluorin was imaged with 488-nm excitation, and fluorescence was collected through a 510-nm longpass filter and a 40$\times$ N.A. 1.25 objective. Images were collected at a rate of 1 image per minute. Neurons were continuously perfused at the flowing rate of $\approx$1 ml/min into a round chamber (1.1-cm diameter) with an extracellular buffer containing 140 mM NaCl, 3 mM KCl, 2 mM $CaCl_2$, 2 mM $MgCl_2$, 10 mM Hepes, 20 mM glucose, and 0.5 μM TTX (pH 7.3). The composition of NMDA perfusion solution was similar to that of extracellular buffer except that it also contained 300 μM $MgCl_2$, 20 μM NMDA, and 10 μM glycine. Images were collected for 5 min to establish a baseline (F_0) before perfusion with NMDA solution for 5 min. Subsequently, neurons were continuously perfused with extracellular buffer to monitor fluorescence recovery. Images were analyzed using National Institutes of Health ImageJ software. Changes of average fluorescence intensity were manually traced to compensate for x–y shift and are expressed as $\Delta F/F_0$.

ACKNOWLEDGMENTS. We thank Louise Lucast for the generation of critical reagents and advice; Xuelin Lou, Shawn Ferguson, and Gilbert Di Paolo for critical readings of the manuscript; and James Howe for discussion. We also thank Da-Ting Lin and Richard Huganir (The Johns Hopkins University, Baltimore, MD) for the gift of the pH-GluR2 constructs and for advice on their usage in imaging experiments. This work was supported in part by the G. Harold and Leila Y. Mathers Charitable Foundation and National Institutes of Health Grants NS36251, CA46128, DK45735, and DA018343 (to P.D.C.).

1. Dingledine R, Borges K, Bowie D, Traynelis SF (1999) The glutamate receptor ion channels. *Pharmacol Rev* 51:7–61.
2. Song I, Huganir RL (2002) Regulation of AMPA receptors during synaptic plasticity. *Trends Neurosci* 25:578–588.
3. Bredt DS, Nicoll RA (2003) AMPA receptor trafficking at excitatory synapses. *Neuron* 40:361–379.
4. Passafaro M, Piech V, Sheng M (2001) Subunit-specific temporal and spatial patterns of AMPA receptor exocytosis in hippocampal neurons. *Nat Neurosci* 4:917–926.
5. Malinow R, Malenka RC (2002) AMPA receptor trafficking and synaptic plasticity. *Annu Rev Neurosci* 25:103–126.
6. Sheng M, Kim MJ (2002) Postsynaptic signaling and plasticity mechanisms. *Science* 298:776–780.
7. Carroll RC, *et al.* (1999) Dynamin-dependent endocytosis of ionotropic glutamate receptors. *Proc Natl Acad Sci USA* 96:14112–14117.
8. Burbea M, Dreier L, Dittman JS, Grunwald ME, Kaplan JM (2002) Ubiquitin and AP180 regulate the abundance of GLR-1 glutamate receptors at postsynaptic elements in C. elegans. *Neuron* 35:107–120.
9. Kastning K, *et al.* (2007) Molecular determinants for the interaction between AMPA receptors and the clathrin adaptor complex AP-2. *Proc Natl Acad Sci USA* 104:2991–2996.
10. Granseth B, Odermatt B, Royle SJ, Lagnado L (2006) Clathrin-mediated endocytosis is the dominant mechanism of vesicle retrieval at hippocampal synapses. *Neuron* 51:773–786.
11. Murthy VN, De Camilli P (2003) Cell biology of the presynaptic terminal. *Annu Rev Neurosci* 26:701–728.
12. Gray NW, *et al.* (2003) Dynamin 3 is a component of the postsynapse, where it interacts with mGluR5 and Homer. *Curr Biol* 13:510–515.
13. Perez-Otano I, *et al.* (2006) Endocytosis and synaptic removal of NR3A-containing NMDA receptors by PACSIN1/syndapin1. *Nat Neurosci* 9:611–621.
14. Cremona O, *et al.* (1999) Essential role of phosphoinositide metabolism in synaptic vesicle recycling. *Cell* 99:179–188.
15. McPherson PS, *et al.* (1996) A presynaptic inositol-5-phosphatase. *Nature* 379:353–357.
16. Harris TW, Hartwieg E, Horvitz HR, Jorgensen EM (2000) Mutations in synaptojanin disrupt synaptic vesicle recycling. *J Cell Biol* 150:589–600.
17. Dickman DK, Horne JA, Meinertzhagen IA, Schwarz TL (2005) A slowed classical pathway rather than kiss-and-run mediates endocytosis at synapses lacking synaptojanin and endophilin. *Cell* 123:521–533.
18. Di Paolo G, De Camilli P (2006) Phosphoinositides in cell regulation and membrane dynamics. *Nature* 443:651–657.
19. Zoncu R, *et al.* (2007) Loss of endocytic clathrin-coated pits upon acute depletion of phosphatidylinositol 4,5-bisphosphate. *Proc Natl Acad Sci USA* 104:3793–3798.
20. Perera RM, Zoncu R, Lucast L, De Camilli P, Toomre D (2006) Two synaptojanin 1 isoforms are recruited to clathrin-coated pits at different stages. *Proc Natl Acad Sci USA* 103:19332–19337.
21. Hayashi M, *et al.* (2008) Cell- and stimulus-dependent heterogeneity of synaptic vesicle endocytic recycling mechanisms revealed by studies of dynamin 1-null neurons. *Proc Natl Acad Sci USA* 105:2175–2180.
22. Mani M, *et al.* (2007) The dual phosphatase activity of synaptojanin1 is required for both efficient synaptic vesicle endocytosis and reavailability at nerve terminals. *Neuron* 56:1004–1018.
23. Guo S, Stolz LE, Lemrow SM, York JD (1999) SAC1-like domains of yeast SAC1, INP52, and INP53 and of human synaptojanin encode polyphosphoinositide phosphatases. *J Biol Chem* 274:12990–12995.
24. Nemoto Y, *et al.* (2001) Identification and characterization of a synaptojanin 2 splice isoform predominantly expressed in nerve terminals. *J Biol Chem* 276:41133–41142.
25. Cestra G, *et al.* (1999) The SH3 domains of endophilin and amphiphysin bind to the proline-rich region of synaptojanin 1 at distinct sites that display an unconventional binding specificity. *J Biol Chem* 274:32001–32007.
26. Slepnev VI, De Camilli P (2000) Accessory factors in clathrin-dependent synaptic vesicle endocytosis. *Nat Rev Neurosci* 1:161–172.
27. Itoh T, *et al.* (2005) Dynamin and the actin cytoskeleton cooperatively regulate plasma membrane invagination by BAR and F-BAR proteins. *Dev Cell* 9:791–804.
28. Cestra G, Toomre D, Chang S, De Camilli P (2005) The Abl/Arg substrate ArgBP2/nArgBP2 coordinates the function of multiple regulatory mechanisms converging on the actin cytoskeleton. *Proc Natl Acad Sci USA* 102:1731–1736.
29. McPherson PS, Kay BK, Hussain NK (2001) Signaling on the endocytic pathway. *Traffic* 2:375–384.
30. McPherson PS, Takei K, Schmid SL, De Camilli P (1994) p145, a major Grb2-binding protein in brain, is co-localized with dynamin in nerve terminals where it undergoes activity-dependent dephosphorylation. *J Biol Chem* 269:30132–30139.
31. Irie F, Okuno M, Pasquale EB, Yamaguchi Y (2005) EphrinB-EphB signalling regulates clathrin-mediated endocytosis through tyrosine phosphorylation of synaptojanin 1. *Nat Cell Biol* 7:501–509.
32. Berman DE, *et al.* (2008) Oligomeric amyloid-beta peptide disrupts phosphatidylinositol-4,5-bisphosphate metabolism. *Nat Neurosci* 11:547–554.
33. Auger C, Marty A (1997) Heterogeneity of functional synaptic parameters among single release sites. *Neuron* 19:139–150.
34. Turrigiano GG, Nelson SB (2004) Homeostatic plasticity in the developing nervous system. *Nat Rev Neurosci* 5:97–107.
35. Luthi A, *et al.* (2001) Synaptojanin 1 contributes to maintaining the stability of GABAergic transmission in primary cultures of cortical neurons. *J Neurosci* 21:9101–9111.
36. Thiagarajan TC, Lindskog M, Tsien RW (2005) Adaptation to synaptic inactivity in hippocampal neurons. *Neuron* 47:725–737.
37. Murthy VN, Schikorski T, Stevens CF, Zhu Y (2001) Inactivity produces increases in neurotransmitter release and synapse size. *Neuron* 32:673–682.
38. Ramjaun AR, McPherson PS (1996) Tissue-specific alternative splicing generates two synaptojanin isoforms with differential membrane binding properties. *J Biol Chem* 271:24856–24861.
39. Miesenbock G, De Angelis DA, Rothman JE (1998) Visualizing secretion and synaptic transmission with pH-sensitive green fluorescent proteins. *Nature* 394:192–195.
40. Lin DT, Huganir RL (2007) PICK1 and phosphorylation of the glutamate receptor 2 (GluR2) AMPA receptor subunit regulates GluR2 recycling after NMDA receptor-induced internalization. *J Neurosci* 27:13903–13908.
41. Shi S, Hayashi Y, Esteban JA, Malinow R (2001) Subunit-specific rules governing AMPA receptor trafficking to synapses in hippocampal pyramidal neurons. *Cell* 105:331–343.
42. Haucke V (2005) Phosphoinositide regulation of clathrin-mediated endocytosis. *Biochem Soc Trans* 33:1285–1289.
43. Rusk N, *et al.* (2003) Synaptojanin 2 functions at an early step of clathrin-mediated endocytosis. *Curr Biol* 13:659–663.
44. Lu J, *et al.* (2007) Postsynaptic positioning of endocytic zones and AMPA receptor cycling by physical coupling of dynamin-3 to Homer. *Neuron* 55:874–889.
45. Shepherd JD, *et al.* (2006) Arc/Arg3.1 mediates homeostatic synaptic scaling of AMPA receptors. *Neuron* 52:475–484.
46. Lee SY, Wenk MR, Kim Y, Nairn AC, De Camilli P (2004) Regulation of synaptojanin 1 by cyclin-dependent kinase 5 at synapses. *Proc Natl Acad Sci USA* 101:546–551.
47. Beattie EC, *et al.* (2000) Regulation of AMPA receptor endocytosis by a signaling mechanism shared with LTD. *Nat Neurosci* 3:1291–1300.
48. Horne EA, Dell'Acqua ML (2007) Phospholipase C is required for changes in postsynaptic structure and function associated with NMDA receptor-dependent long-term depression. *J Neurosci* 27:3523–3534.
49. Hsieh H, *et al.* (2006) AMPAR removal underlies Abeta-induced synaptic depression and dendritic spine loss. *Neuron* 52:831–843.
50. Voronov S, *et al.* (2008) Synaptojanin 1-linked phosphoinositide dyshomeostasis and cognitive deficits in mouse models of Down's syndrome. *Proc Natl Acad Sci USA* 105:9415–9420.
51. Di Paolo G, *et al.* (2004) Impaired PtdIns(4,5)P2 synthesis in nerve terminals produces defects in synaptic vesicle trafficking. *Nature* 431:415–422.